Chemical Geology 493 (2018) 478–490

Contents lists available at ScienceDirect

Chemical Geology

journal homepage: www.elsevier.com/locate/chemgeo

Hypoxia in the Holocene Baltic Sea: Comparing modern versus past intervals using sedimentary trace metals

Niels A.G.M. van Helmond[a,*], Tom Jilbert[a,b], Caroline P. Slomp[a]

[a] Department of Earth Sciences, Faculty of Geosciences, Utrecht University, Princetonlaan 8a, 3584, CB, Utrecht, Netherlands
[b] Ecosystems and Environment Research Program, Faculty of Biological and Environmental Sciences, University of Helsinki, Finland

ARTICLE INFO

Editor: K. Johannesson

Keywords:
Redox conditions
Anthropogenic pollution
Aqueous trace metal depletion
Molybdenum
Uranium

ABSTRACT

Anthropogenic nutrient input has caused a rapid expansion of bottom water hypoxia in the Baltic Sea over the past century. Two earlier intervals of widespread hypoxia, coinciding with the Holocene Thermal Maximum (HTM_{HI}; 8–4 ka before present; BP) and the Medieval Climate Anomaly (MCA_{HI}; ~1200–750 years BP), have been identified from Baltic Sea sediments. Here we present sediment records from two sites in the Baltic Sea, and compare the trace metal (As, Ba, Cd, Cu, Mo, Ni, Pb, Re, Sb, Tl, U, V, Zn) enrichments during all three hypoxic intervals. Distinct differences are observed between the intervals and the various elements, highlighting the much stronger perturbation of trace metal cycles during the modern hypoxic interval. Both Mo and U show a strong correlation with C_{org} and very high absolute concentrations, indicative of frequently euxinic bottom waters during hypoxic intervals. During the modern hypoxic interval ($Modern_{HI}$) comparatively less Mo is sequestered relative to C_{org} than in earlier intervals. This suggests partial drawdown of the water column Mo inventory in the modern water column due to persistent euxinia and only partial replenishment of Mo through North Sea inflows. Molybdenum contents in modern sediments are likely also affected by the recent slowdown in input of Mo in association with deposition of Fe and Mn oxides. Strong enrichments of U in recent sediments confirm that the $Modern_{HI}$ is more intense than past intervals. These results suggest that U is a more reliable indicator for the intensity of bottom water deoxygenation in the Baltic Sea than Mo. Sedimentary Re enrichment commences under mildly reducing conditions, but this element is not further enriched under more reducing conditions. Enrichments of V are relatively minor for the MCA_{HI} and $Modern_{HI,}$ possibly due to strong reservoir effects on V in the water column, indicating that V is unreliable as an indicator for the intensity of bottom water hypoxia in this setting. Furthermore, Ba profiles are strongly influenced by post-depositional remobilization throughout the Holocene. The strong relationship between C_{org} and Ni, Tl and particularly Cu suggests that these trace metals can be used to reconstruct the C_{org} flux into the sediments. Profiles of As, Sb and Cd and especially Pb and Zn are strongly influenced by anthropogenic pollution.

1. Introduction

Sedimentary trace metal records have widely been used as proxies for productivity and redox conditions in both modern and ancient aquatic systems (e.g. Calvert and Pedersen, 1993; Morford and Emerson, 1999; Tribovillard et al., 2006; Brumsack, 2006). Sedimentary trace metal concentrations are often low under a well-oxygenated water column (e.g. McLennan, 2001), while under low-oxygen conditions their concentrations are generally elevated due to the interplay of several related processes (e.g. Tribovillard et al., 2006).

Trace metals are closely associated with organic material in both the water column and in sediments (e.g. Pedersen and Calvert, 1990; Canfield, 1994; Tribovillard et al., 2006). Under well-ventilated conditions, only a fraction of the organic-bound trace metals in the water column reaches the sediment-water interface, due to efficient remineralization of organic matter in the water column. Under low-oxygen conditions, however, less organic material is remineralized leading to an increase in the direct input of organic-bound metals to the sediments. Sediments are further enriched in trace metals under these conditions through uptake of trace metals by organic matter at the sediment-water interface.

A second key vector of trace metal transport to sediments is via Mn- and Fe(oxyhydr)oxides. Many trace metals are adsorbed onto oxide particles, which are highly mobile in seafloor environments where variable redox conditions lead to repeated cycles of dissolution and re-precipitation (e.g. Froelich et al., 1979; Shaw et al., 1990; Tribovillard

* Corresponding author.
E-mail addresses: n.vanhelmond@uu.nl (N.A.G.M. van Helmond), c.p.slomp@uu.nl (C.P. Slomp).

https://doi.org/10.1016/j.chemgeo.2018.06.028
Received 13 April 2018; Received in revised form 25 June 2018; Accepted 29 June 2018
Available online 03 July 2018

et al., 2006). These processes can lead to the focusing of trace metals into defined areas of the seafloor (e.g. Lenz et al., 2015a). Although trace metal enrichment may occur under well-oxygenated conditions when metal-bearing Mn- and Fe-oxides are preserved in the sediments (e.g. Schaller et al., 2000), a more common route of enrichment is that metals are released during dissolution of oxides in the surface sediments, and subsequently sequestered in organic matter, sulfide minerals or other reduced authigenic phases (Morford and Emerson, 1999; Tribovillard et al., 2006).

A third pathway for trace metal enrichment is related to diffusive transport from seawater into sediments and subsequent sequestration in association with organic matter or authigenic minerals. Depending on the metal, enrichment may commence at various stages of bottom water oxygen depletion, i.e. the metal may be sequestered under hypoxic (dissolved oxygen concentrations < 2 mg/l), anoxic (no dissolved oxygen) or euxinic conditions (no dissolved oxygen and presence of free sulfide) (Crusius et al., 1996; Tribovillard et al., 2006; Olson et al., 2017).

Two of the most studied and widely applied redox-sensitive trace metals, Mo and U, have many properties in common (see Algeo and Tribovillard, 2009 for an overview). One key difference between Mo and U is that the presence of free sulfide is a prerequisite for Mo enrichment in sediments. Sulfide is required to convert relatively unreactive seawater molybdate to particle reactive thiomolybdate (Helz et al., 1996). In contrast, authigenic U sequestration, primarily precipitated as uraninite (UO_2), already commences when Fe (III) is reduced to Fe (II) (Zheng et al., 2002), making U a potentially more sensitive recorder of minor changes in bottom water oxygen conditions. Another key difference is that water column Mo is actively scavenged by particle Mn- (and sometimes Fe) oxides, which may carry Mo to the sediment-water interface (e.g. Turekian, 1977; Adelson et al., 2001; Sulu-Gambari et al., 2017), whereas U is generally enriched via diffusion into sediments (e.g. Klinkhammer and Palmer, 1991). These differences in the sequestration of Mo and U can be used for detailed reconstructions of depositional conditions (Algeo and Tribovillard, 2009). In addition, the strong relation between C_{org} and Mo in euxinic environments can be used to identify basin reservoir effects, i.e. the depletion of an element in the water column of a stagnant basin through removal of that specific element to the sediment in excess of resupply by deepwater renewal. In this manner, aqueous Mo may become depleted, resulting in lower sedimentary Mo/C_{org} ratios (Algeo and Lyons, 2006).

Besides Mo and U, Re and V are the most studied and widely used redox-sensitive trace metals (e.g. Morford and Emerson, 1999; Morford et al., 2005). The low crustal abundance of Re results in relatively large, and therefore very distinctive, authigenic enrichments under reducing conditions (Koide et al., 1986; Crusius et al., 1996; Böning et al., 2004). Unlike for instance Mo, Re does not show an affinity for Mn- and Fe-oxides and is sequestered in sediments under suboxic conditions after diffusion across the sediment-water interface (e.g. Colodner et al., 1993; Morford et al., 2012). Under well-oxygenated conditions V (in the form of vanadate oxyanions) adsorbs onto Mn- and Fe-oxides (e.g. Wehrli and Stumm, 1989), but is also strongly associated with organic matter (e.g. Beck et al., 2008), so both may be important carriers of V to deeper waters or the sediment-water interface. Under moderately reducing conditions, V(V) is reduced to V(IV), which is more surface reactive and more easily complexes with (in)organic ligands (Emerson and Huested, 1991). This may lead to enhanced sedimentary V sequestration, but the complexation of V(IV) with dissolved organic matter may also allow it to remain in the aqueous phase (e.g. O'Connor et al., 2015; Olson et al., 2017). In contrast with for instance Mo, V sequestration is not linked to the formation of authigenic sulfides (Algeo and Maynard, 2004). However, under euxinic conditions V can be reduced to V(III), which enables V sequestration through the precipitation of vanadium(hydr)oxide (Wanty and Goldhaber, 1992).

A prime example, and perhaps the most widely used trace metal to reconstruct marine primary productivity, is sedimentary Ba, which largely reflects biogenic barite ($BaSO_4$), a remnant of decayed organic matter that is preserved in sediments (Bishop, 1988; Dymond et al., 1992; Schoepfer et al., 2015). The applicability of sedimentary Ba as a (paleo)productivity proxy seems to be limited to open ocean settings, for example, because a certain water depth (~1000 m) is needed in order to fully develop the barite-productivity signal settings (Von Breymann et al., 1992; Plewa et al., 2012). Its applicability is further complicated by remobilization of Ba under reducing conditions (e.g. McManus et al., 1998; Henkel et al., 2012). Despite these complications Ingri et al. (2014) showed that sedimentary Ba may represent primary productivity in the Bothnian Bay during the last 5.5 kyr.

Furthermore, trace metal enrichments are also used to assess anthropogenic pollution in (semi)modern sediments (e.g. Caccia et al., 2003; Ip et al., 2007). Many trace metals have applications in agriculture and industry, e.g. in fertilizers, pesticides, pigments and lubricants. These trace metals can be transported to the oceans by fluvial and eolian pathways, where they are sequestered in sediments after adsorption onto clay particles and (oxyhydr)oxides and complexation with organic compounds (e.g. Nriagu and Pacyna, 1988; Windom et al., 1989; Liaghati et al., 2004).

The Baltic Sea is an ideal location to assess how changes in bottom water oxygen, primary productivity and anthropogenic pollution are recorded by trace metals in marine sediments. Its geographic configuration, i.e. landlocked with a restricted connection to the open ocean (Fig. 1a), in combination with excessive anthropogenic nutrient input (e.g. Gustafsson et al., 2012), has resulted in a tenfold increase of the hypoxic area over the past century (Carstensen et al., 2014), creating the world's largest human-induced “dead zone” (Diaz and Rosenberg, 2008). The modern Baltic hypoxic interval (henceforth $Modern_{HI}$), was preceded by two previous hypoxic intervals during the Holocene (Zillén et al., 2008). The first hypoxic interval coincided with the Holocene Thermal Maximum (HTM_{HI}; ~8 and 4 ka before present - BP). The second interval of widespread hypoxia in the Baltic Sea coincided with the Medieval Climate Anomaly (MCA_{HI}; ~1200–750 years BP).

The laminated sediments marking the hypoxic intervals in the Baltic Sea are characterized by high organic carbon (C_{org}) and molybdenum (Mo) contents (Jilbert and Slomp, 2013a; Dijkstra et al., 2016; Hardisty et al., 2016; Papadomanolaki et al., 2018), indicative of free sulfide in bottom waters (Helz et al., 1996). Previous studies have drawn various conclusions about the environmental conditions during each of the hypoxic intervals. High-resolution records of Mo enrichment indicate that the development of the $Modern_{HI}$ was more rapid than the development of the MCA_{HI} and HTM_{HI}, while the maximum intensity of hypoxia was similar for all three events (Jilbert and Slomp, 2013a). In contrast, Hardisty et al. (2016) concluded, based on Mo isotopes, that reducing conditions during the MCA_{HI} and HTM_{HI} were probably more intense than during the $Modern_{HI}$. Focusing on the areal extent, rather than intensity, of hypoxia, Lenz et al. (2015a) concluded on the basis of sedimentary Fe records that the present-day hypoxic area is larger than that in the past.

Here we present a comprehensive analysis of trace metal enrichments during the three hypoxic intervals from two sites in the central Baltic Sea. By considering a large number of trace metals together, we are able to test multiple hypotheses about the mechanisms of trace metal enrichment, and the suitability of trace metals for paleoenvironmental reconstructions in this setting. Specifically, we investigate (1) the sensitivity of known redox-sensitive trace metal enrichments, i.e. Mo, U, Re and V, to variable redox conditions, (2) which trace metals may be reliable proxies for the organic carbon (C_{org}) flux into the sediments and (3) the effect of anthropogenic pollution on sedimentary trace metal records. We have generated complete discrete-sample records of 13 trace metals (As, Ba, Cd, Cu, Mo, Ni, Pb, Re, Sb, Tl, U, V, Zn), as well as major and minor sediment components (Al, Fe, S, C_{org}), for the entire sediment column spanning the three hypoxic intervals and the intervening oxic periods, at two sites in the Baltic Sea (Fig. 1).

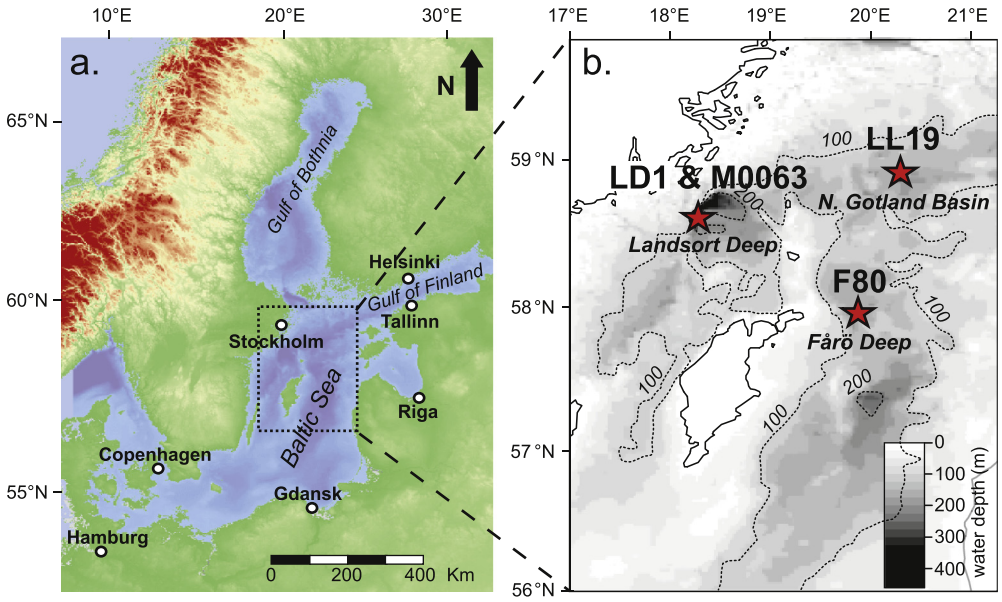

Fig. 1. Bathymetric map of the Baltic Sea generated at www.helcom.fi (a). Detailed bathymetric map of the central part of the Baltic Sea, with our study sites F80 and LL19 and the sites brought forward in the discussion, LD1 & M0063 (Lenz et al., 2015b; Dijkstra et al., 2016; Hardisty et al., 2016), marked by a red star (b). Map modified from Jilbert and Slomp (2013a). (For interpretation of the references to colour in this figure legend, the reader is referred to the web version of this article.)

Additionally, we present Laser Ablation–Inductively Coupled Plasma–-Mass Spectrometry (LA-ICP-MS) line-scan Mo and U data for the three intervals at one of the two study sites. The LA-ICP-MS records allow an orders-of-magnitude increase in the depth resolution of the trace metal profiles, facilitating robust analysis of relative enrichments between Mo and U, and investigation of how the two elements respond to short-timescale changes in oxygen conditions.

2. Materials and methods

2.1. Study site

Sediment samples were retrieved from two different localities in the central part of the Baltic Sea during two research cruises with *R/V Aranda* in May–June 2009 and August 2013. Multicores (0–35 cm below seafloor; cmbsf) and gravity cores (~25–440 cmbsf) were collected from site F80 in the Fårö Deep (58.0000°N, 19.8968°E, 191 m water depth) and from site LL19 in the Northern Gotland Basin (58.8807°N, 20.3108°E, 169 m water depth; Fig. 1) in 2009. An additional short core (0–55 cmbsf) was taken at site F80 in 2013 with a GEMAX corer.

2.2. Processing of the sediment cores

The multicores and GEMAX core were sliced on board the ship under an oxygen-free atmosphere at in-situ bottom water temperature. The resolution of the sediment slices was 0.5 cm for 0–2 cmbsf, 1 cm for 2–10 cmbsf and 2 cm from 10 cmbsf until the bottom of the core. The GEMAX core for F80 retrieved in 2013 was sliced under the same conditions but with a resolution of 1 cm for the samples analysed in this study (0–10 cmbsf). The gravity cores were stored at 4 °C and sliced under an oxygen-free atmosphere in the laboratory at Utrecht University at a resolution of 1 cm. All sediment samples were freeze-dried and weighed before and after freeze-drying in order to determine the water content and to calculate porosity. The samples were subsequently powdered and homogenized using an agate mortar and pestle in an oxygen-free atmosphere.

2.3. Organic carbon content

Organic carbon content data (C_{org}) for the 2009 cores was generated and published by Jilbert and Slomp (2013a). For the 2013 GEMAX core 0.1–0.2 g of freeze-dried and powdered sediment sample was weighed in 15 ml centrifuge tubes and 7.5 ml of 1 M HCl was added to dissolve carbonates. After 4 h on a shaker the acid was removed through centrifugation and fresh 1 M HCl was added after which the samples were left on a shaker overnight. The acid was then removed again after centrifugation and samples were washed twice with milliQ water, and dried at 60 °C for 72 h. The dried residues were then weighed again to determine the weight loss. Finally, the samples were powdered and homogenized and ~5 mg of each sample was weighed in a tinfoil cup. Total carbon analyses were performed using a Fisons Instruments NA 1500 NCS analyzer. Obtained results were normalized to in-house standards, acetanilide, atropine and nicotinamide. An internationally certified soil standard (IVA2) was measured after each 10 samples to determine the accuracy and precision of our analyses. The certified value for IVA2 is 0.732 wt% C, our obtained mean value was 0.726 wt% C with a standard deviation of 0.014 wt% C. Finally, C_{org} was calculated upon correction for the weight loss due to the decalcification. An average analytical uncertainty of 0.08 wt% was calculated based on duplicate analyses of sediment samples.

2.4. Trace metal concentrations

For the determination of sedimentary trace metal concentrations about 125 mg of freeze-dried and powdered sediment sample was weighed in 30 ml Teflon vessels. Subsequently 2.5 ml of mixed acid ($HClO_4$:HNO_3, 3:2) and 2.5 ml 40% HF were added and the vessels were left overnight on a hotplate at 90 °C. The following day the lids of the vessels were removed and the extracts were heated to 140 °C to evaporate the acids. The remaining residues were then dissolved in 25 ml 4.5% HNO_3 and left overnight on a hotplate at 90 °C again. The dilution of the final solutions was determined by weighing the vessels, after which the solutions were analysed by Inductively Coupled Plasma-Optical Emission Spectrometry (ICP-OES; Al, Fe and S published previously in Jilbert and Slomp (2013a) and Lenz et al. (2015a)) and by Inductively Coupled Plasma-Mass Spectometry (ICP-MS; As, Cd, Cu, Mo, Ni, Pb, Re, Sb, Tl, U, V and Zn). For the latter analyses, we used an XSeries II ICP-MS (Thermo Fisher Scientific) equipped with a Peltier cooled, low-volume conical spray chamber fitted with a micro nebulizer, a micro pump and a FAST system on the autosampler (SC-4 DX; Elemental Scientific), to enhance stability, enable fast washout and minimum cross contamination and optimize sample throughput. The accuracy (recovery) was generally between 95 and 105% for all

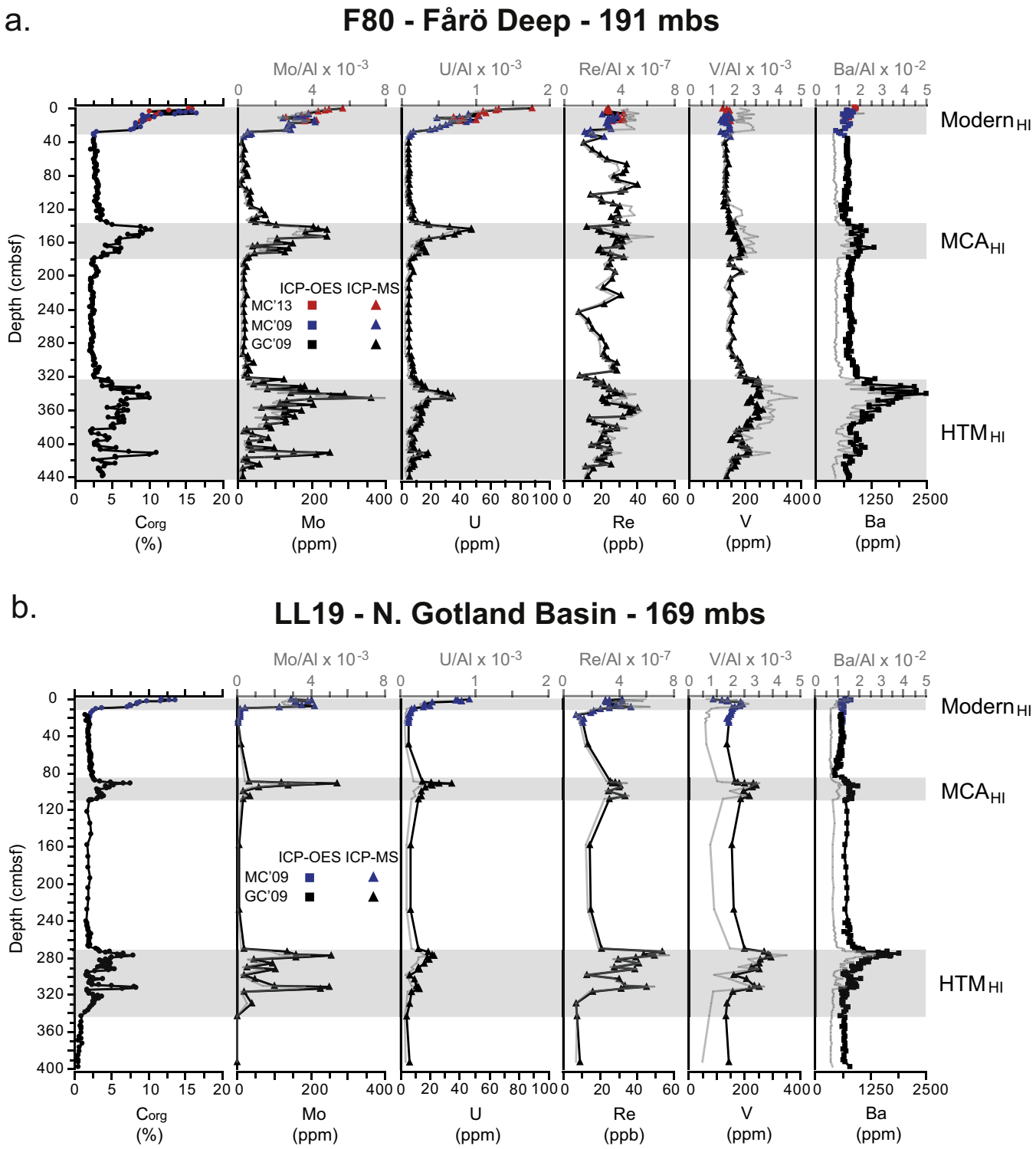

Fig. 2. Profiles of C_{org}, Mo, Mo/Al, U, U/Al, Re, Re/Al, V, V/Al, Ba and Ba/Al, for F80 (a.) and LL19 (b.) plotted against depth. Grey bars indicate the three hypoxic intervals in the Baltic Sea: the modern hypoxic interval ($Modern_{HI}$), the hypoxic interval during the Medieval Climate Anomaly (MCA_{HI}) and the hypoxic interval during the Holocene Thermal Maximum (HTM_{HI}). The data for the multicores collected in 2009 (MC'09) are represented by blue symbols, while the data for the GEMAX core collected in 2013 (MC'13) are represented by red symbols. The data for gravity cores collected in 2009 (GC'09) are represented by black symbols. (For interpretation of the references to colour in this figure legend, the reader is referred to the web version of this article.)

reported elements based on in-house standards. The average analytical uncertainty based on duplicates, in-house standards and laboratory reference material (ISE-921) was 2% for As, 1% for Cd, 2% for Cu, 1% for Mo, 2% for Ni, 2% for Pb, 8% for Re, 2% for Sb, 4% for Tl, 2% for U, 2% for V and 2% for Zn.

2.5. Resin embedding and LA-ICP-MS

Sections of the sediment cores from F80 (2009 gravity core and 2013 GEMAX core) were prepared for LA-ICP-MS analysis by resin embedding. From the gravity core, U-channels of sediment

(20 × 2 × 1 cm) were sampled horizontally from the open core surface as described in Jilbert et al. (2008) and transferred immediately to an N_2-filled glovebox. A total of 180 cm of sediment, including the laminated intervals corresponding to the MCA_{HI} and HTM_{HI}, were sampled in this way. From the GEMAX core, a vertical column of miniature sub-cores of sediment (8 sub-cores in total, each 1 cm diameter, 7 cm length) was taken as described in Jilbert and Slomp (2013a). The entire sub-coring operation was performed in a N_2-filled glove bag and the sub-cores were transferred to an N_2-filled glovebox. All U-channels and sub-cores were then dehydrated with argon-purged acetone, fixed in Spurr's epoxy resin, and sliced to reveal the interior surface using a water-cooled rock saw. The interior surfaces were polished prior to subsequent analysis.

Resin-embedded sediment blocks were mounted in the ablation chamber of the LA-ICP-MS instrument at Utrecht University. The ablation chamber sits on a mobile stage. Line scan profiles were generated by focusing a pulsed argon-fluoride excimer laser beam (120 μm spot size, 193 nm wavelength, 10 Hz repetition rate, 8 J cm^{-2} energy density) onto the moving sample surface and ablating material into a high mass-resolution ICP-MS (Thermo Element 2) via a He-Ar carrier gas. During line scans the stage velocity was optimized to 0.0275 mm s^{-1} for high spatial resolution measurements (Hennekam et al., 2015). Count rates of the isotopes ^{27}Al, ^{98}Mo and ^{238}U, among a range of other elements, were determined continuously at a measurement frequency of approximately 1 Hz.

The resin embedding procedure results in varying degrees of sediment compaction, such that the length of each line scan is less than that of the original U-channel or sub-core. To correct for compaction effects, the data from each LA-ICP-MS line scan was linearly re-scaled to the initial length of the sub-core. Subsequently, line scan data were fine-tuned by alignment to ICP-OES or ICP-MS data of discrete samples from the corresponding interval.

Raw LA-ICP-MS count data were converted to elemental compositional ratios via the two-step linear calibration procedure described in Jilbert and Slomp (2013a). Briefly, count rates of each element in the line-scan data were converted to preliminary concentrations using one-point sensitivity factors (counts/ppm) determined from a glass standard (NIST 610) at equivalent measurement settings. Preliminary concentrations of ^{98}Mo and ^{238}U were then normalized to ^{27}Al to correct for variable ablation yield during line scanning. The resulting ratios, corrected for natural isotopic abundances of each element, were further corrected using a linear regression against Mo/Al and U/Al concentration ratios of the equivalent sediment interval determined by discrete sample ICP-OES or ICP-MS analysis. This second step corrects for any offset between the sensitivity factors of the elements in the sediment sample relative to the standard glass.

2.6. Sediment chronologies

Age-depth models for the sediment cores used in this study were previously generated by Jilbert and Slomp (2013a) and Lenz et al. (2015a). For the present study we choose to show our data against depth instead of time. We have, however, included the dates, following Lenz et al. (2015a), in the Supplementary data file. We follow Jilbert and Slomp (2013a) concerning the position of the $Modern_{HI}$, MCA_{HI} and the HTM_{HI}. For the purposes of this study we do not discern different sub-events within the MCA_{HI} and HTM_{HI}.

3. Results

3.1. Trace metals in the Fårö Deep (site F80) and Northern Gotland Basin (site LL19)

The hypoxic intervals in the Fårö Deep are characterized by strong enrichments in sedimentary C_{org} (Fig. 2a). Maximum values are similar (~10 wt%; Table 1) for the three hypoxic events when the top sediments consisting of fresh, non-degraded organic material, the so-called "fluffy" layer, are left out of consideration. Both Mo and U are also strongly enriched in the sediments of all three hypoxic intervals (Fig. 2a; Table 1). Maximum values for Mo (> 300 ppm) are recorded during the HTM_{HI}. Background Mo concentrations, i.e. in the intervening oxic intervals, are 25 ppm on average (Table 1). Uranium concentrations progressively increase from the HTM_{HI} to the $Modern_{HI}$, hence the present-day U concentration is the highest in the record. In contrast with C_{org}, Mo and U, Re shows rather constant concentrations throughout the studied sediment sequence, without significant enrichments during the hypoxic intervals (Fig. 2a; Table 1). Both V and Ba are strongly enriched during the HTM_{HI}, but not during other intervals, in particular the $Modern_{HI}$.

Table 1
Average (avg.) and maximum (max.) values for C_{org}, Mo, U, Re, V, Ba, Zn, Pb, Sb, As, Cd, Ni, Tl, Cu, Fe, S for the three hypoxic intervals and background at site F80.

	$Modern_{HI}$[a]		MCA_{HI}		HTM_{HI}		Background	
	Avg.	Max.	Avg.	Max.	Avg.	Max.	Avg.	Max.
C_{org} (wt%)	8.4 (10.3)	11.6 (16.4)	6.1	10.3	5.3	11.1	2.6	3.8
Mo (ppm)	151 (169)	212 (283)	120	242	109	360	25	73
U (ppm)	34 (41)	52 (88)	21	47	13	35	5.8	8.2
Re (ppb)	24 (24)	32 (32)	26	34	23	40	24	40
V (ppm)	133 (133)	152 (152)	167	194	210	262	148	191
Ba (ppm)	686 (723)	862 (938)	940	1326	1131	2498	761	959
Zn (ppm)	747 (728)	1100 (1100)	147	182	136	154	142	249
Pb (ppm)	100 (92)	146 (146)	32	54	24	32	31	48
Sb (ppm)	11 (12)	16 (16)	2.3	3.6	3.2	8.2	1.7	5.3
As (ppm)	49 (49)	68 (68)	16	23	21	46	12.3	26.3
Cd (ppm)	9.1 (9.0)	15.1 (15.1)	1.9	3.3	1.7	3.8	0.5	1.2
Ni (ppm)	96 (100)	115 (124)	65	89	73	107	54	61
Tl (ppm)	3.1 (3.1)	4.7 (4.7)	1.8	2.8	1.9	3.0	1.1	1.6
Cu (ppm)	184 (198)	232 (296)	100	173	102	206	46	62
Fe (wt%)	4.8 (4.5)	7.0 (7.0)	7.0	8.7	6.3	8.6	5.9	7.8
S (wt%)	2.0 (1.8)	3.8 (3.8)	4.5	7.0	3.5	6.8	1.6	4.0

[a] $Modern_{HI}$ including the not yet compacted and degraded surface sediments rich in fresh organic matter the so-called "fluffy" layer between brackets.

The profiles of C_{org} and trace metals for the Northern Gotland Basin site LL19 (Fig. 2b) largely resemble those for the Fårö Deep (Fig. 2a). Maximum C_{org} values for the three hypoxic intervals are slightly lower than in the Fårö Deep, i.e. around 8 wt% (Fig. 2b; Table 2). Maximum values for Mo are recorded during the MCA_{HI} and HTM_{HI}, with somewhat lower maximum values during the $Modern_{HI}$ (Fig. 2b). However, background Mo concentrations in the intervening oxic intervals (~6 ppm) are much lower than in the Fårö Deep (Tables 1 and 2). Absolute U concentrations are also lower in the sediments of the Northern Gotland Basin, but the trend in U concentrations is the same as for the Fårö Deep, i.e. progressively increasing in the order HTM_{HI}–MCA_{HI}–$Modern_{HI}$. In contrast with the Fårö Deep, distinct enrichments in Re are observed during all three hypoxic intervals in the Northern Gotland Basin (Fig. 2b). Moreover, background Re concentrations in the intervening oxic intervals (10 ppb) are generally lower than in the Fårö Deep. Again, both V and Ba are strongly enriched during the HTM_{HI}, but strong enrichments are absent from the other intervals.

The other trace metals all show their strongest enrichments coinciding with the onset of the $Modern_{HI}$ (Fig. 3a). Significant enrichment in Zn is entirely confined to the $Modern_{HI}$, while for Pb there is also a small enrichment towards the end of the MCA_{HI}, followed by a rapid drop and a gradual increase towards the $Modern_{HI}$ (Fig. 3a). For Sb and As we observe both a strong $Modern_{HI}$-related enrichment and moderate enrichments during both the MCA_{HI} and HTM_{HI}, which generally follow the profiles of S and Fe (Fig. 3a). Enrichments in Cd, Ni, Tl and

Table 2
Average (avg.) and maximum (max.) values for C_{org}, Mo, U, Re, V, Ba, Zn, Pb, Sb, As, Cd, Ni, Tl, Cu, Fe, S for the three hypoxic intervals and background at site LL19.

	$Modern_{HI}$[a]		MCA_{HI}		HTM_{HI}		Background	
	Avg.	Max.	Avg.	Max.	Avg.	Max.	Avg.	Max.
C_{org} (wt%)	6.7 (8.4)	9.8 (13.7)	3.8	7.5	3.5	8.4	1.8	2.5
Mo (ppm)	112 (135)	210 (210)	106	271	100	255	6	11
U (ppm)	17 (24)	41 (46)	19	34	13	23	6	7
Re (ppb)	25 (26)	36 (36)	28	34	31	54	11	15
V (ppm)	168 (154)	192 (192)	205	242	225	294	147	160
Ba (ppm)	619 (660)	675 (820)	777	964	920	1893	647	914
Zn (ppm)	606 (549)	1092 (1092)	159	190	139	150	163	208
Pb (ppm)	81 (69)	135 (135)	35	45	27	29	37	44
Sb (ppm)	12 (12)	20 (20)	3.5	6.4	3.4	6.4	1.6	3.0
As (ppm)	44 (42)	79 (79)	30	39	31	52	17	23
Cd (ppm)	5.9 (6.1)	11.9 (11.9)	1.8	3.1	1.1	2.1	0.4	0.8
Ni (ppm)	98 (97)	127 (127)	71	93	76	114	53	56
Tl (ppm)	1.9 (2.0)	3.3 (3.3)	1.6	2.4	1.6	2.3	1.1	1.4
Cu (ppm)	109 (131)	179 (191)	86	152	81	130	42	54
Fe (wt%)	6.6 (6.0)	10.0 (10.0)	6.1	7.4	5.8	7.4	5.5	6.9
S (wt%)	2.9 (2.6)	6.9 (6.9)	2.4	5.0	2.1	4.3	1.1	2.4

[a] $Modern_{HI}$ including the not yet compacted and degraded surface sediments rich in fresh organic matter the so-called “fluffy” layer between brackets.

Cu are more similar to those of C_{org} and Mo. Even the smaller variations in C_{org} and Mo, e.g. the maximum around 410 cmbsf (Fig. 3a), are clearly expressed, and the absolute magnitude of the enrichments in Ni, Tl and Cu is rather similar for all three of the hypoxic events.

As for the Fårö Deep, significant enrichment in Zn in the Northern Gotland Basin is confined to the $Modern_{HI}$, while for Pb there is also a small enrichment visible towards the end of the MCA_{HI}. For Sb, As, Cd, Ni Tl, and Cu, there are, besides the strong $Modern_{HI}$-related enrichment, clear enrichments visible during both the MCA_{HI} and HTM_{HI} (Fig. 3b). The magnitude of the enrichments in Ni, Tl and Cu is again similar for the three different hypoxic intervals, while for Sb, As and Cd, the enrichment during the $Modern_{HI}$ is much larger than the enrichments during the MCA_{HI} and HTM_{HI} (Fig. 3b).

3.2. High-resolution molybdenum and uranium records

Trends in the high-resolution Mo and U LA-ICP-MS data for each of the hypoxic intervals in the Fårö Deep (Fig. 4) are in good agreement with the results for the discrete samples (Fig. 2a). However, the LA-ICP-MS data reveal significantly more internal variability within these intervals, and rapid changes in enrichment as previously demonstrated by Jilbert and Slomp (2013a) for shorter sections of the Holocene record. Moreover, the LA-ICP-MS data clearly show that U enrichment increases gradually at the onset of centennial-scale ‘hypoxic events’ within the hypoxic intervals (zoom sections labeled ‘onset’ in Fig. 4). In contrast, Mo enrichments increase rapidly beyond a certain point in the development of each event.

The contrast between relative Mo and U enrichments in each hypoxic interval is further illustrated by the LA-ICP-MS data. Although both elements are clearly enriched in all intervals, the Mo/U ratio differs markedly between HTM_{HI}, MCA_{HI} and $Modern_{HI}$. In hypoxic events within HTM_{HI}, Mo/U oscillates around 10, while in MCA_{HI} the average value is close to 5, and for $Modern_{HI}$ the average value is close to 3.5 (Fig. 4).

4. Discussion

4.1. Molybdenum and uranium as proxies of bottom water redox conditions

The extremely high concentrations of Mo during the three hypoxic intervals can only be explained by persistent euxinic conditions at these times (e.g. Scott and Lyons, 2012), as concluded by previous studies of Baltic Sea sediments (Jilbert and Slomp, 2013a; Dijkstra et al., 2016). The similar maximum values of C_{org} and Mo for the three hypoxic intervals have previously been interpreted to indicate that the intensity of hypoxia during each interval was similar (Jilbert and Slomp, 2013a). However, the increase in U concentrations from the HTM_{HI} to the $Modern_{HI}$ observed in our new data causes us to reassess this conclusion. Taken alone, the U records suggest that the intensity of the hypoxic intervals has in fact increased towards the present day. This would imply that increased anthropogenic nutrient inputs to the Baltic during the 20th century (e.g. Gustafsson et al., 2012; Carstensen et al., 2014) have led to a perturbation of trace metal cycling that exceeds the natural variability observed in earlier hypoxic intervals.

The average background Mo concentration of 25 ppm in the Fårö Deep suggests that even outside the hypoxic intervals, bottom waters in this location may have been intermittently euxinic (Scott and Lyons, 2012). The lower average background Mo concentration in the Northern Gotland Basin (6 ppm), although substantially above the crustal average (~1–2 ppm; McLennan, 2001), is significantly below that of the Fårö Deep, suggesting that sulfide remained restricted to pore waters (Scott and Lyons, 2012). This difference can be attributed to the greater water depth of the Fårö Deep (191 m versus 169 m), making it naturally more susceptible to deoxygenation. The relatively early onset of U enrichment compared to Mo during short-timescale hypoxic events within the HTM_{HI}, MCA_{HI} and $Modern_{HI}$ in the Fårö Deep (Fig. 4) is likely related to the fact that sedimentary U enrichment via the reduced phase UO_2 commences in the zone of Fe oxide reduction (Zheng et al., 2002). Whereas Mo enrichment via thiomolybdates requires the presence of free sulfide (Helz et al., 1996). During the onset of a hypoxic event, progressive stagnation of deep water masses may have resulted in a staggered timing of U and Mo enrichment. However, once a hypoxic event is initiated, the two elements show strongly correlated patterns of enrichment on short timescales (see coincident peaks in Fig. 4). We note that this interpretation implies that sedimentary U and Mo contents are determined by processes that occur very close to the sediment-water interface.

4.2. Drawdown of water column molybdenum

The regression slope between sedimentary Mo and C_{org} content has been shown to differ between modern (intermittently) hypoxic marine basins as a function of the degree of restriction of the sub-chemocline water mass (Algeo and Lyons, 2006). The Mo/C_{org} ratio has been successfully applied as a proxy to determine extent of water mass restriction in marine basins during for example the Mesozoic Oceanic Anoxic Events (e.g. McArthur et al., 2008; van Helmond et al., 2014), and also to study past hypoxia in the Baltic Sea (Jilbert and Slomp, 2013a). The latter study showed that the Mo/C_{org} data for both the Northern Gotland Basin and the Fårö Deep during the MCA_{HI} and HTM_{HI} plot close to the regression slope for (semi)modern sediments from Saanich Inlet, considered to be the least restricted of the four modern euxinic basins studied by Algeo and Lyons (2006) with a deep water renewal period of ~1.5 years. Therefore Jilbert and Slomp (2013a) concluded that the basin reservoir effect in the Baltic Sea was negligible. Our new datasets show (Fig. 5a, b), that the Mo/C_{org} data for the $Modern_{HI}$ plot considerably below the Mo/C_{org} data for the MCA_{HI} and HTM_{HI}. The regression line would have been even more flat if the “fluffy-layer” had been included as well because of the relatively high C_{org} content in this top layer (open symbols in Fig. 5a, b). The flatter regression line for Mo/C_{org} during the $Modern_{HI}$ implies partial drawdown of the water column Mo inventory, and thus the potential impact of a basin reservoir effect on sedimentary Mo data. A basin reservoir effect may have important implications, for example, for the interpretation of $\delta^{98}Mo$ records from the Baltic Sea (e.g. Hardisty et al., 2016). Based on these findings we conclude that U is a more reliable indicator of bottom water

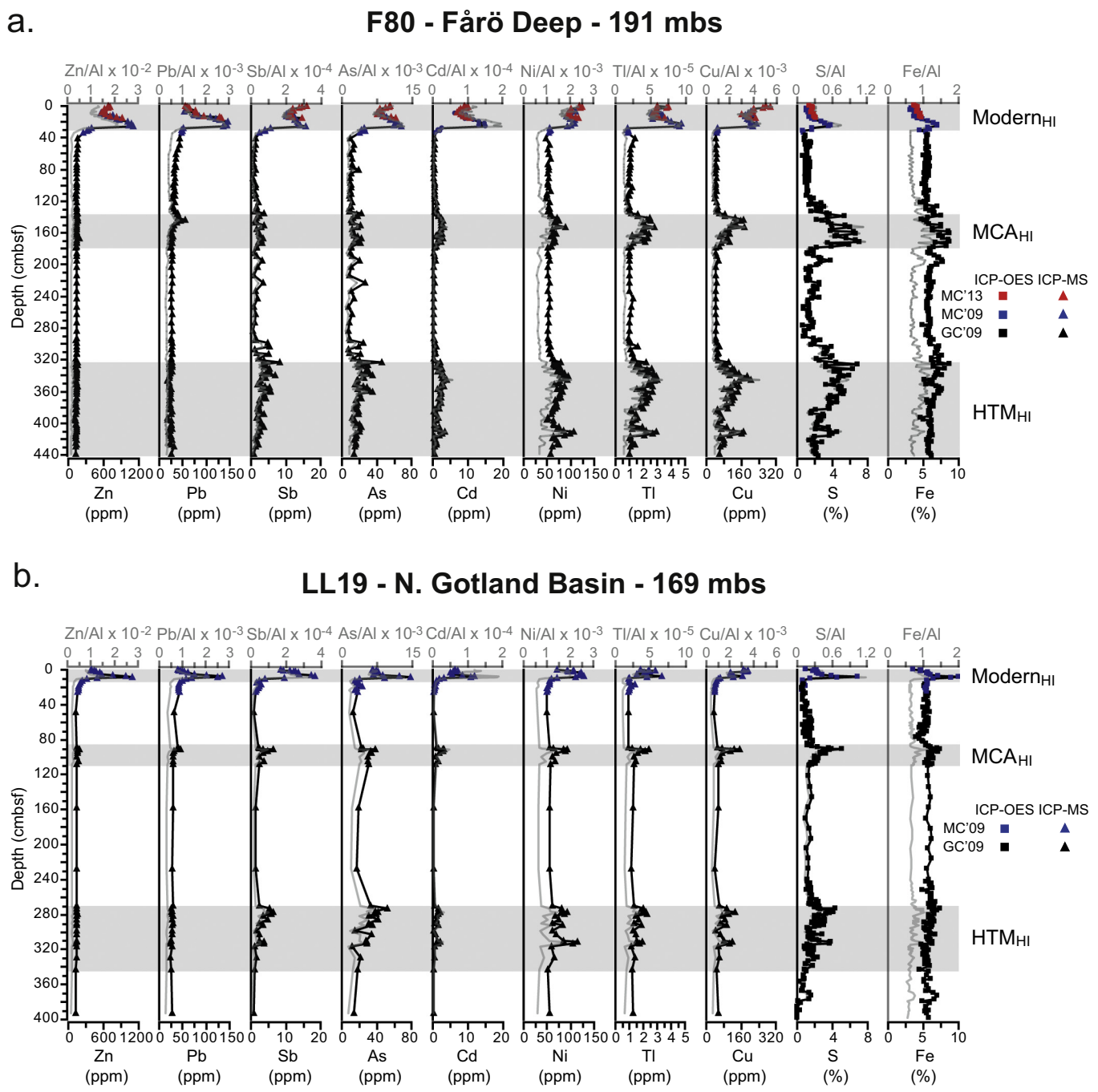

Fig. 3. Profiles of Zn, Zn/Al, Pb, Pb/Al, Sb, Sb/Al, As, As/Al, Cd, Cd/Al, Ni, Ni/Al, Tl, Tl/Al, Cu, Cu/Al, S, S/Al, Fe and Fe/Al for F80 (a.) and LL19 (b.) plotted against depth. Grey bars indicate the three hypoxic intervals in the Baltic Sea: the modern hypoxic interval ($Modern_{HI}$), the hypoxic interval during the Medieval Climate Anomaly (MCA_{HI}) and the hypoxic interval during the Holocene Thermal Maximum (HTM_{HI}). The data for multicores collected in 2009 (MC'09) are represented by blue symbols, while those for the GEMAX core collected in 2013 (MC'13) are represented by red symbols. The data for gravity cores collected in 2009 (GC'09) are represented by black symbols. (For interpretation of the references to colour in this figure legend, the reader is referred to the web version of this article.)

hypoxia intensity than Mo in the Baltic Sea and potentially also in other euxinic basins affected by a reservoir effect.

Both the Northern Gotland Basin and Fårö Deep are located in the central part of the Baltic Proper, in the pathway followed by episodically occurring Major Baltic Inflows (MBIs; Matthäus and Franck, 1992; Lass and Matthäus, 1996). These MBIs introduce large quantities of relatively high-saline and well-oxygenated North Sea waters into the Baltic Sea following meteorological events (e.g. Schinke and Matthäus, 1998). The relatively high density of the waters introduced during MBIs leads to bottom water ventilation (e.g. Mohrholz et al., 2015). Besides oxygen, the North Sea waters contain trace metals, thereby potentially replenishing the water column Mo inventory. However, not all MBIs penetrate into the more remote sub-basins of the Baltic Sea, such as the Landsort Deep (Mohrholz et al., 2015). Hence, the sub-basins further downstream along the path of the MBIs may be expected to show longer residence times and thus comparatively severe drawdown of water column Mo during hypoxic intervals. To test this hypothesis, we compiled Mo/C_{org} data for the three hypoxic intervals in the Landsort Deep ($Modern_{HI}$ - Lenz et al., 2015b, site LD1; MCA_{HI} and HTM_{HI} - Dijkstra et al., 2016, IODP exp. 347 site M0063; Fig. 1). The cross-plot of Mo

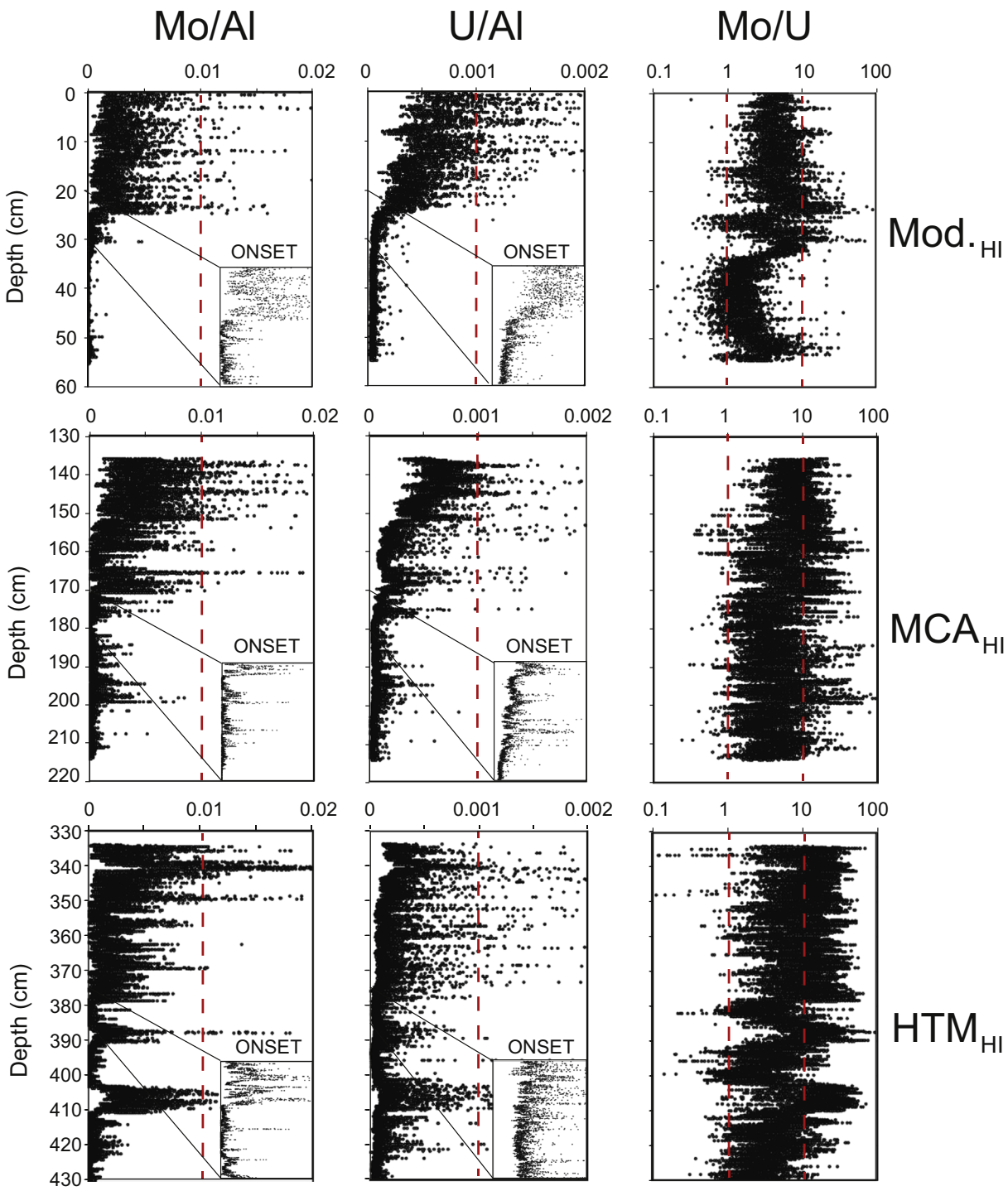

Fig. 4. High-resolution, Laser Ablation–Inductively Coupled Plasma–Mass Spectrometry (LA-ICP-MS) Mo/Al, U/Al and Mo/U profiles for the three hypoxic intervals in the Baltic Sea for F80: the modern hypoxic interval ($Modern_{HI}$), the hypoxic interval during the Medieval Climate Anomaly (MCA_{HI}) and the hypoxic interval during the Holocene Thermal Maximum (HTM_{HI}).

and C_{org} data for the Landsort Deep shows relatively flat regression slopes for all three the hypoxic events (Fig. 5c). In contrast with the data for the Northern Gotland Basin and the Fårö Deep and a previous study for the Landsort Deep by Hardisty et al. (2016), this suggests that there was water column Mo depletion in the Landsort Deep during all three hypoxic intervals. Our explanation is supported by the relatively low concentrations of aqueous Mo throughout the water column in both the Gotland Deep and the Landsort Deep (Nägler et al., 2011; Noordmann et al., 2015; Bauer et al., 2017).

The $Modern_{HI}$ developed more rapidly than any past event of hypoxia in the Baltic Sea during the Holocene (Jilbert and Slomp, 2013a). This more rapid development of hypoxia may have contributed to drawdown of water column Mo. Furthermore, the water exchange between the Baltic Sea and the North Sea has decreased over the last 8 kyr (e.g. Gustafsson and Westman, 2002), leading to the relatively long modern residence time for water in the Baltic Sea (~30 years; e.g. Döös et al., 2004), thereby increasing the chance for water column Mo drawdown to occur. Finally, the present-day hypoxic and euxinic area is

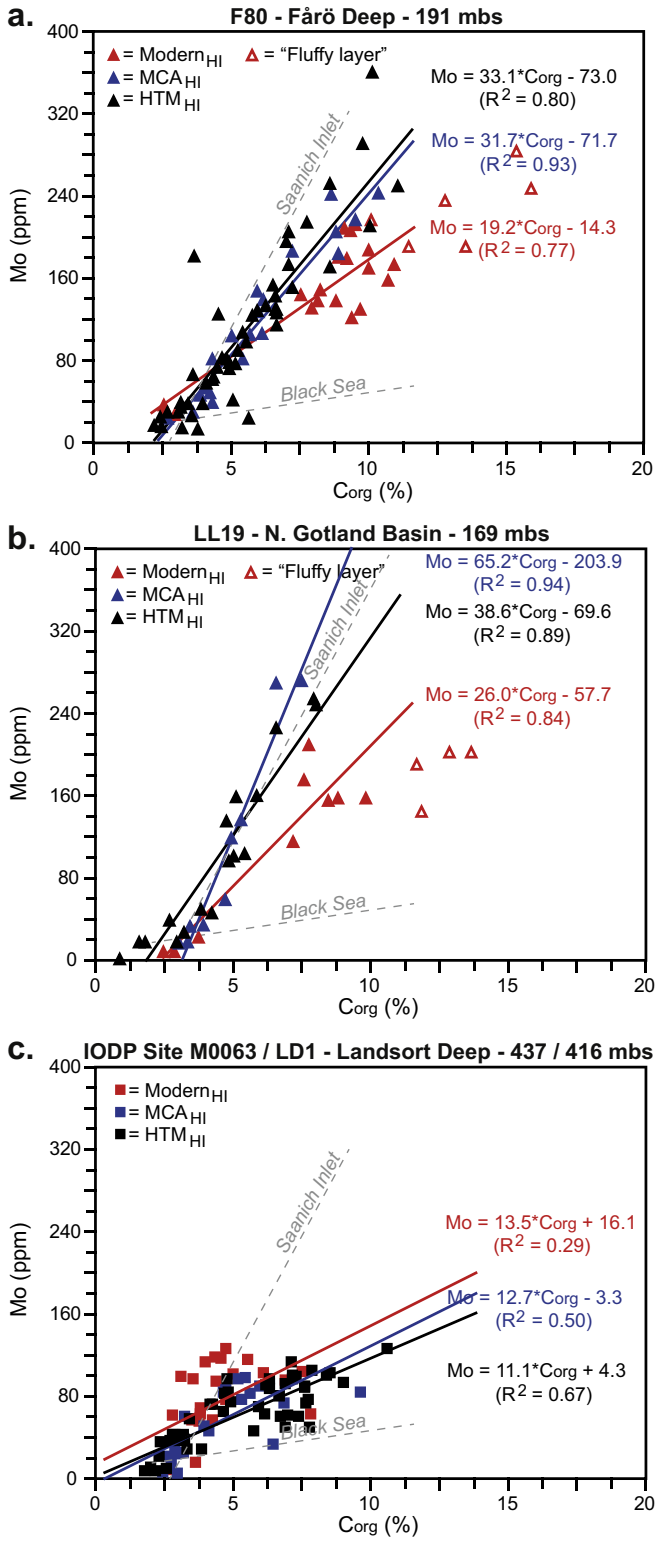

Fig. 5. Cross-plots of sedimentary Mo versus C_{org} for F80 (a), LL19 (b) and the Landsort Deep (IODP exp. 347 Site M0063; Dijkstra et al., 2016 – MCA_{HI} and HTM_{HI} and LD1; Lenz et al., 2015b – $Modern_{HI}$) for the three hypoxic intervals in the Baltic Sea: the modern hypoxic interval ($Modern_{HI}$; red), the hypoxic interval during the Medieval Climate Anomaly (MCA_{HI}; blue) and the hypoxic interval during the Holocene Thermal Maximum (HTM_{HI}; black). Solid lines represent regression slopes for sedimentary Mo versus C_{org}. For the calculation of the regression slopes samples from the surface "fluffy layer" were excluded. The dashed lines show the regression slopes for sedimentary Mo versus C_{org} for the weakly restricted Saanich Inlet and the severely restricted Black Sea (Algeo and Lyons, 2006). (For interpretation of the references to colour in this figure legend, the reader is referred to the web version of this article.)

large (e.g. Carstensen et al., 2014), and hypoxia is not only confined to the deeper parts of the basin but is also widely present in shelf and coastal areas (Conley et al., 2011; Lenz et al., 2015a). These hypoxic shelf and coastal areas, e.g. in the Belt Seas, the Finnish Archipelago Sea, the Gulf of Finland and the Stockholm Archipelago, cover thousands of square kilometers, substantially increasing, the area in the Baltic Sea where Mo is potentially sequestered, when compared to the deeper parts of the basin alone. The amount of Mo sequestered in these shelf and coastal areas is limited, however (Jokinen et al., 2018), since they are generally only seasonally hypoxic and only sporadically euxinic (e.g. Conley et al., 2011). However, during the HTM_{HI} large parts of the, present-day well-ventilated, Bothnian Sea were still hypoxic (e.g. Zillén et al., 2008) and potentially even euxinic (Jilbert et al., 2015), suggesting that the hypoxic and euxinic area may have been equally large or even larger during the HTM_{HI}. We therefore suggest that the rapid development of the $Modern_{HI}$, in combination with decreasing water exchange between the open ocean and the Baltic Sea, has led to the observed lower sedimentary Mo sequestration and implied drawdown of the water column Mo inventory.

Cross-plots of the enrichment factors of Mo and U from the discrete sample analyses show (Fig. 6) that the depositional system in the Baltic Sea is characterized by an active oxide particulate shuttle, comparable with for instance the Cariaco Basin (Algeo and Tribovillard, 2009). The active oxide particulate shuttle in the Baltic Sea leads to generally elevated Mo/U values relative to unrestricted marine anoxic settings (Fig. 6), because in contrast with U, Mo is actively scavenged by particle Mn- (and sometimes Fe) oxides, which may carry Mo to the sediment-water interface, thereby enhancing its sequestration potential (e.g. Turekian, 1977; Adelson et al., 2001; Sulu-Gambari et al., 2017). However, samples from the $Modern_{HI}$ plot towards the upper boundary of, or outside, the particulate shuttle zone identified by Algeo and Tribovillard (2009), indicating a shift towards lower Mo/U as also seen in the LA-ICP-MS data (Fig. 4), and as observed in other anoxic basins (Algeo and Tribovillard, 2009). We suggest that at our study sites in the Baltic Sea, this evolution is a direct result of the decline in the rate of Fe and Mn particulate shuttling in recent decades due to hypoxia, as demonstrated by Lenz et al. (2015a). Lower Fe and Mn particle shuttling will have reduced the supply of Mo to our study sites (e.g. Turekian, 1977; Adelson et al., 2001; Sulu-Gambari et al., 2017), contributing to the observed trends in sedimentary Mo (Figs. 2, 4, 5).

4.3. Rhenium and vanadium as proxies of bottom water redox conditions

Authigenic Re sequestration occurs under suboxic, relatively mildly reducing conditions (Crusius et al., 1996; Morford et al., 2005). Our results confirm that Re is a sensitive recorder of mildly reducing conditions, particularly because of its large enrichment factor relative to crustal average values (Koide et al., 1986). The sedimentary Re profiles of the Fårö Deep and Northern Gotland Basin show large differences, which we attribute to the different background redox conditions for the two studied sites. The relatively reducing background conditions in the Fårö Deep caused a (nearly) continuously sequestration of Re throughout the studied interval (i.e. during the last ~7 kyr; Jilbert and Slomp, 2013a), while in the Northern Gotland Basin conditions for enhanced Re sequestration were only reached during the three hypoxic intervals. The lack of further enrichment during the more intensely reducing conditions of the HTM_{HI}, MCA_{HI} and $Modern_{HI}$, suggests that sedimentary Re concentrations are not useful as a quantitative proxy for the intensity of hypoxia in the central Baltic Sea. The contemporaneous presence of sulfide and Re in pore waters implies that sedimentary Re sequestration is not enhanced by the presence of sulfide (e.g. Colodner et al., 1993; Olson et al., 2017). Therefore, enrichment of Re does not accelerate as the intensity of reducing conditions increases within the hypoxic interval.

Vanadium is one of the most widely used trace metals to reconstruct paleoredox conditions and generally shows strong sedimentary

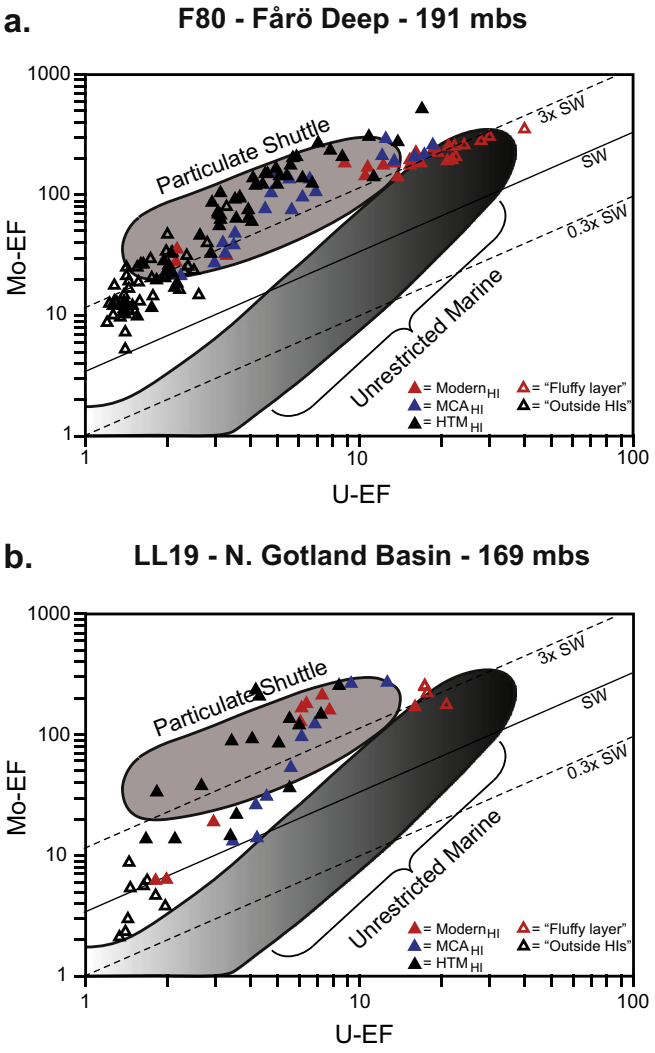

Fig. 6. Cross-plots of the enrichment factors (EF), following Algeo and Tribovillard (2009) and Tribovillard et al. (2012), of Mo and U for F80 (a) and LL19 (b) plotted on a logarithmic scale. The shaded areas represent the types of environment in which sediments with such composition are deposited, i.e. a system characterized by an active particulate shuttle like the Cariaco Basin or an unrestricted marine system such as the eastern tropical Pacific (Algeo and Tribovillard, 2009; Tribovillard et al., 2012). The diagonal lines represent multiples of the Mo:U ratio in present-day seawater. Molar ratios of ~7.5 for the Pacific and ~7.9 for the Atlantic have been converted to an average weight ratio of 3.1 for the purpose of comparison with sediment Mo:U weight ratios (cf. Tribovillard et al., 2012).

enrichments under reducing conditions, with relative enrichments similar to those found for Mo and U (e.g. Algeo and Maynard, 2004; Tribovillard et al., 2006). The sedimentary V records presented in this study are, however, very different from the records for Mo and U. Particularly the absence of (strong) enrichments during the Modern$_{HI}$ is striking (Fig. 2).

The absence of (strong) enrichments in V might theoretically be related to complexation of V with dissolved organic matter under reducing conditions (Brumsack and Gieskes, 1983; Beck et al., 2008). The formation of dissolved metal-organic complexes leads to retention of V in pore waters and the consequent absence of sedimentary V enrichments (e.g. O'Connor et al., 2015; Olson et al., 2017). The problem with this explanation for the records presented here is that C_{org} concentrations for the three hypoxic intervals are very similar, so large differences in dissolved organic matter concentrations between the hypoxic intervals are not expected. The effect of complexation of V with dissolved organic matter should therefore have been similar for the three hypoxic intervals. The type of organic matter and the degree to which it has decayed may, however, also be of importance. Particularly the degree of decay of organic matter is probably very different for the Modern$_{HI}$ and MCA$_{HI}$ compared to the HTM$_{HI}$.

An alternative explanation for the unexpected V profiles might be found in variations in the strength of the particulate shuttle. Water column vanadate adsorbs onto Mn- and Fe(oxyhydr)oxides (e.g. Wehrli and Stumm, 1989; Morford et al., 2005), which can then carry V to deeper areas, thereby increasing the potential for sedimentary V sequestration. The more muted Fe shuttle during the Modern$_{HI}$ (Lenz et al., 2015a), could therefore be a reason for the absence of sedimentary V enrichments during the Modern$_{HI}$. Again however, this interpretation cannot fully explain the V profiles, since the rate of shuttling was significantly higher during the MCA$_{HI}$ - as indicated by strong enrichments of Fe and S at this time (Fig. 2) - but V enrichments were similarly low to those in the Modern$_{HI}$.

Two studies of water column V concentrations in the modern Baltic Sea demonstrated a significant depletion (> 60%) of this element relative to conservative mixing of freshwater and seawater (Prange and Kremling, 1985; Bauer et al., 2017). Prange and Kremling (1985) also showed V depletion to be significantly greater than Mo or U depletion (which were effectively conservative with respect to seawater mixing at the studied locations), and attributed this effect to the particle reactivity of seawater vanadate during mixing in the turbid waters of the Baltic Sea. In addition, the V that enters the Baltic Sea via riverine pathways is already (partly) removed upon estuarine mixing (Prange and Kremling, 1985). These observations imply that V in the Baltic Sea is subject to an even greater reservoir effect than Mo, and hence that the sedimentary record of V enrichment may be strongly impacted by basin-wide drawdown of water column V. As described above for Mo (Section 4.2), the reservoir effect is more likely to be activated during the recent hypoxic intervals (MCA$_{HI}$ and Modern$_{HI}$) than during the HTM$_{HI}$, due to the lower replenishment rate of seawater vanadate in the late Holocene bathymetric configuration of the Baltic. This would explain why the MCA$_{HI}$ and Modern$_{HI}$ show strongly muted V enrichments relative to the HTM$_{HI}$ (Fig. 2).

4.4. The potential of trace metal concentrations as a proxy for primary productivity in the Baltic Sea

Sedimentary Ba concentrations are widely used as a proxy for productivity (e.g. Bishop, 1988; Dymond et al., 1992; Schoepfer et al., 2015). The Ba profiles in this study are, however, unrelated to C_{org} (Fig. 2; with the exception of the maximum during the HTM$_{HI}$), suggesting that Ba profiles in the Baltic Sea are generally not a reliable proxy for productivity. It is well-known that sedimentary Ba records may be strongly overprinted by remobilization and diagenetic precipitation of barite ($BaSO_4$). Particularly in environments with a shallow sulfate-methane transition zone (SMTZ) below which sulfate concentrations drop below saturation with respect to barite, remobilization and diagenetic precipitation of barite occurs (Henkel et al., 2012). This mechanism can also impact the Ba profiles observed in the Fårö Deep and Northern Gotland Basin (Fig. 2). The relatively low salinity of the Baltic Sea, in combination with high rates of methane production in the organic-rich sediments, has led to the formation of a shallow SMTZ (~20 cmbsf; e.g. Jilbert and Slomp, 2013b). This configuration favors the remobilization of Ba after accumulation as biogenic barite, partially erasing the original enrichment and smoothing the sedimentary Ba profile. Additionally, barite reprecipitation fronts are often observed close to the SMTZ (Dickens, 2001), fed by an upwards flux of dissolved Ba in the porewaters.

The barium profiles at F80 and LL19 show strong enrichments close to the termination of the HTM$_{HI}$, but relatively muted enrichments during the rest of the record (Fig. 2). The maximum Ba values close to the termination of the HTM$_{HI}$ correlate with maxima in C_{org}, Mo and U

and therefore ostensibly suggest a strong productivity maximum at this time. However, the anomalously high concentrations lead us to propose that Ba in this interval was also supplemented by the formation of a barite reprecipitation front. Although the SMTZ at the onset of the HTM_{HI} was likely deeper than today due to the higher salinity of the Baltic at this time (Gustafsson and Westman, 2002; Egger et al., 2017), its position must have migrated upwards during the HTM_{HI} itself in response to the loading of organic matter. Indeed, the strong Mo enrichments of the HTM_{HI} indicate significant levels of free sulfide in pore waters at this time, consistent with a relatively shallow SMTZ. Hence, a barite reprecipitation front likely established at the SMTZ during the HTM_{HI} as per the model of Dickens (2001). The HTM_{HI} persisted for > 3000 years (Jilbert and Slomp, 2013a), during which an organic-rich sediment layer of at least 80–100 cm accumulated (Fig. 2). Assuming barite in this layer to be continually remobilized and reprecipitated close to the SMTZ, it follows that the inventory of reprecipitated Ba for the HTM_{HI} should be significantly greater than that for the later hypoxic intervals of much shorter duration (MCA_{HI} and $Modern_{HI}$). Hence, no equivalent peak is observed at the termination of the MCA_{HI} or in the modern SMTZ. We note that loss of Ba to the water column after barite dissolution in the SMTZ is unlikely during any of the hypoxic intervals, due to the persistent presence of pore water sulfate close to the sediment-water interface (Jilbert and Slomp, 2013b).

As outlined in Section 4.1, Mo and U enrichments are strongly related to bottom water redox conditions. However, both elements also correlate well with C_{org}, due to the close relationship between productivity and oxygen depletion in the Baltic Sea, and thus serve as indirect proxies for past productivity. Various other trace elements show similarly strong correlations with C_{org}, which may be more closely related to direct input to sediments in association with organic material. These include Ni, Tl and particularly Cu (Fig. 3). Both Ni and Cu behave as micronutrients in oxic marine environments and are scavenged in the water column and enriched in sediments through complexation with organic matter (e.g. Calvert and Pedersen, 1993; Piper and Perkins, 2004), while Cu is also actively scavenged by Mn- and Fe-oxides (Fernex et al., 1992). Enrichments in sedimentary Ni and Cu have been previously suggested as indicators of higher primary productivity (e.g., Piper and Perkins, 2004; Tribovillard et al., 2006). Our Cu and Ni records suggest that this interpretation is valid for the Baltic Sea. Moreover, Tl shows a strong similarity with Cu and Ni, suggesting that these three elements may be the most suitable trace metals to be applied as proxies for the C_{org} flux to the sediments in the Baltic Sea. The similarity of enrichments of As and Sb to those of Fe and S, on the other hand (Fig. 3) shows that these elements may be more strongly influenced by the rate of shelf-to-basin Fe shuttling.

4.5. Trace metals as an indicator of anthropogenic pollution

Besides the enhanced input of nutrients responsible for the modern eutrophication of the Baltic Sea (Gustafsson et al., 2012; Carstensen et al., 2014), anthropogenic activity has also led to enhanced input of trace metals (e.g. Kremling and Streu, 2000). These anthropogenically derived trace metals have entered the surface waters of the Baltic Sea via riverine and atmospheric pathways in dissolved and particulate forms (Schneider et al., 2000), resulting in widespread trace metal enrichments in surface sediments of the Baltic Sea (e.g. Borg and Jonsson, 1996; Szefer et al., 1996). Enrichments of Zn, Pb, Sb, As, Cd, Ni, Tl and Cu in our data are significantly higher during the $Modern_{HI}$ than during the MCA_{HI} and HTM_{HI}, confirming the strong anthropogenic signal in the recent sediments. Although industrialization in the Baltic Sea region was intense from the Second World War onwards, most trace metal enrichments at F80 and LL19 show a rapid onset at the start of the $Modern_{HI}$, which has been tied to the year 1979 (Lenz et al., 2015b). We attribute this delayed response to a combination of factors. Firstly, because most of these metals are sequestered as authigenic sulfides (e.g. Tribovillard et al., 2006), the hypoxic conditions of the $Modern_{HI}$, were required before significant accumulation at F80 and LL19 could occur. Secondly, it is likely that these metals initially accumulated in association with Fe oxides in shelf areas, before being transported into the deep basins when Fe shuttling accelerated at the start of the $Modern_{HI}$ (Lenz et al., 2015a). Sedimentary trace metal concentrations remain elevated after the onset of the $Modern_{HI}$, but the enrichments are generally less extreme. We attribute this to decreasing anthropogenic input (Kremling and Streu, 2000), as well as a decline in the rate of Fe shuttling since the early part of the $Modern_{HI}$ (Lenz et al., 2015a). The strong effect of recent anthropogenic pollution on the records makes most of these metals unsuitable as quantitative indicators for the intensity of modern hypoxia. A strong anthropogenic overprint does make an element such as Zn, for example, useful as a tool to date recent sediments. Pollution-derived Pb was already used for this purpose (Zillén et al., 2012; van Helmond et al., 2017).

5. Conclusions

The trace metal records from the Baltic Sea presented in this study show that Mo and U are strongly correlated with each other and C_{org}. High concentrations of both trace metals are indicative of frequently euxinic bottom waters during all three hypoxic intervals. High-resolution LA-ICP-MS Mo/U data show that U sequestration generally leads Mo enrichment, which we attribute to the known redox-dependence of authigenic U and Mo sequestration. Crossplots of Mo/C_{org} suggest depletion of aqueous Mo concentrations during the $Modern_{HI}$. We attribute this to the unprecedented rapid development of widespread hypoxia during the $Modern_{HI}$ combined with reduced water exchange with the adjacent North Sea. The muted Mn and Fe oxide particulate shuttle during the last two decades may also contribute to the observed trends in sedimentary Mo by decreasing the supply of Mo to the deep basins of the Baltic Sea. Uranium does not seem to be affected by reservoir and/or shuttling effects. Its maximum concentrations during the $Modern_{HI}$ suggest that reducing conditions in the Baltic Sea are currently more intense than during the proceeding hypoxic intervals. Rhenium and V profiles are very different from Mo and U, indicating that their applicability as a quantitative proxy for redox conditions is limited. Our sedimentary records show that Re enrichment commences under relatively mildly reducing conditions, but that Re is not further enriched under more reducing conditions. Vanadium may experience a significant reservoir effect due to particle reactivity of seawater vanadate in the turbid Baltic Sea, strongly impacting on V sediment records. Besides Mo and U, Ni, Tl and particularly Cu show strong correlation with C_{org}, suggesting that these are the most reliable trace metals to reconstruct the C_{org} flux into the sediments. Barium, in contrast, is largely decoupled from C_{org}. We attribute this decoupling to diagenetic remobilization and precipitation of Ba resulting from a shallow sulfate methane transition zone in the Baltic Sea. Anthropogenic pollution has led to strong enrichments in Pb, Zn, As, Sb, Cd, Ni, Tl and Cu during the $Modern_{HI}$, far exceeding concentrations observed for the previous hypoxic intervals. The profiles for Pb and Zn are dominated by such anthropogenic sources, making these metals useless as quantitative indicators for (paleo)redox and productivity conditions, while facilitating their use as independent age constraints.

Acknowledgements

This research was funded by the Netherlands Organisation for Scientific Research (NWO; Vici grant #865.13.005) and by the European Research Council under the European Community's Seventh Framework Programme (FP7/2007–2013)/ERC Starting Grant #278364. This work was carried out under the program of the Netherlands Earth System Science Center (NESSC), financially supported by the Ministry of Education, Culture and Science (OCW). We thank the captain, crew and scientific participants of both cruises with the *R/V Aranda*, Helen de Waard, Coen Mulder and Arnold van Dijk for

analytical assistance and Susanne Bauer and Thomas Algeo for constructive reviews.

Appendix A. Supplementary data

Supplementary data to this article can be found online at https://doi.org/10.1016/j.chemgeo.2018.06.028.

References

Adelson, J.M., Helz, G.R., Miller, C.V., 2001. Reconstructing the rise of recent coastal anoxia; molybdenum in Chesapeake Bay sediments1. Geochim. Cosmochim. Acta 65 (2), 237–252.

Algeo, T.J., Lyons, T.W., 2006. Mo–total organic carbon covariation in modern anoxic marine environments: implications for analysis of paleoredox and paleohydrographic conditions. Paleoceanography 21, PA1016. http://dx.doi.org/10.1029/2004PA001112.

Algeo, T.J., Maynard, J.B., 2004. Trace-element behavior and redox facies in core shales of Upper Pennsylvanian Kansas-type cyclothems. Chem. Geol. 206, 289–318.

Algeo, T.J., Tribovillard, N., 2009. Environmental analysis of paleoceanographic systems based on molybdenum–uranium covariation. Chem. Geol. 268 (3), 211–225.

Bauer, S., Blomqvist, S., Ingri, J., 2017. Distribution of dissolved and suspended particulate molybdenum, vanadium, and tungsten in the Baltic Sea. Mar. Chem. http://dx.doi.org/10.1016/j.marchem.2017.08.010.

Beck, M., Dellwig, O., Schnetger, B., Brumsack, H.-J., 2008. Cycling of trace metals (Mn, Fe, Mo, U, V, Cr) in deep pore waters of intertidal flat sediments. Geochim. Cosmochim. Acta 72, 2822–2840.

Bishop, J.K.B., 1988. The barite-opal-organic carbon association in oceanic particulate matter. Nature 332, 341–343.

Böning, P., Brumsack, H.-J., Böttcher, M.E., Schnetger, B., Kriete, C., Kallmeyer, J., Borchers, S.L., 2004. Geochemistry of Peruvian near-surface sediments. Geochim. Cosmochim. Acta 68, 4429–4451.

Borg, H., Jonsson, P., 1996. Large-scale metal distribution in Baltic Sea sediments. Mar. Pollut. Bull. 32 (1), 8–21.

Brumsack, H.J., 2006. The trace metal content of recent organic carbon-rich sediments: implications for Cretaceous black shale formation. Palaeogeogr. Palaeoclimatol. Palaeoecol. 232, 344–361.

Brumsack, H.J., Gieskes, J.M., 1983. Interstitial water trace-metal chemistry of laminated sediments from the Gulf of California, Mexico. Mar. Chem. 14 (1), 89–106.

Caccia, V.G., Millero, F.J., Palanques, A., 2003. The distribution of trace metals in Florida Bay sediments. Mar. Pollut. Bull. 46 (11), 1420–1433.

Calvert, S.E., Pedersen, T.F., 1993. Geochemistry of recent oxic and anoxic marine sediments: implications for the geological record. Mar. Geol. 113, 67–88.

Canfield, D.E., 1994. Factors influencing organic carbon preservation in marine sediments. Chem. Geol. 114 (3), 315–329.

Carstensen, J., Andersen, J.H., Gustafsson, B.G., Conley, D.J., 2014. Deoxygenation of the Baltic Sea during the last century. Proc. Natl. Acad. Sci. U. S. A. 111, 5628–5633. http://dx.doi.org/10.1073/pnas.1323156111.

Colodner, D., Sachs, J., Ravizza, G., Turekian, K., Edmond, J., Boyle, E., 1993. The geochemical cycle of rhenium: a reconnaissance. Earth Planet. Sci. Lett. 117, 205–221.

Conley, D.J., Carstensen, J., Aigars, J., Axe, P., Bonsdorff, E., Eremina, T., Haahti, B.M., Humborg, C., et al., 2011. Hypoxia is increasing in the coastal zone of the Baltic Sea. Environ. Sci. Technol. 45, 6777–6783.

Crusius, J., Calvert, S., Pedersen, T., Sage, D., 1996. Rhenium and molybdenum enrichments in sediments as indicators of oxic, suboxic and sulfidic conditions of deposition. Earth Planet. Sci. Lett. 145 (1–4), 65–78.

Diaz, R.J., Rosenberg, R., 2008. Spreading dead zones and consequences for marine ecosystems. Science 321, 926–929. http://dx.doi.org/10.1126/science.1156401.

Dickens, G.R., 2001. Sulfate profiles and barium fronts in sediment on the Blake Ridge: present and past methane fluxes through a large gas hydrate reservoir. Geochim. Cosmochim. Acta 65 (4), 529–543.

Dijkstra, N., Slomp, C.P., Behrends, T., 2016. Vivianite is a key sink for phosphorus in sediments of the Landsort Deep, an intermittently anoxic deep basin in the Baltic Sea. Chem. Geol. 438, 58–72.

Döös, K., Meier, H.E.M., Döscher, R., 2004. The Baltic haline conveyor belt or the overturning circulation and mixing in the Baltic. Ambio 33, 258–262.

Dymond, J., Suess, E., Lyle, M., 1992. Barium in deep-sea sediment: a geochemical proxy for paleoproductivity. Paleoceanography 7 (2), 163–181.

Egger, M., Hagens, M., Sapart, C.J., Dijkstra, N., van Helmond, N.A.G.M., Mogollón, J.M., Risgaard-Petersen, N., van der Veen, C., Kasten, S., Riedinger, N., Böttcher, M.E., Röckmann, T., Jørgensen, B.B., Slomp, C.P., 2017. Iron oxide reduction in methane rich deep Baltic Sea sediments. Geochim. Cosmochim. Acta 207, 256–276. http://dx.doi.org/10.1016/j.gca.2017.03.019.

Emerson, S.R., Huested, S.S., 1991. Ocean anoxia and the concentration of molybdenum and vanadium in seawater. Mar. Chem. 34, 177–196.

Fernex, F., Février, G., Benaïm, J., Arnoux, A., 1992. Copper, lead and zinc trapping in Mediterranean deep-sea sediments: probable coprecipitation with manganese and iron. Chem. Geol. 98, 293–308.

Froelich, P.N., Klinkhammer, G.P., Bender, M.L., Luedtke, N.A., Heath, G.R., Cullen, D., Dauphin, P., Hammond, D., Hartman, B., Maynard, V., 1979. Early oxidation of organic matter in pelagic sediments of the eastern equatorial Atlantic: suboxic diagenesis. Geochim. Cosmochim. Acta 43, 1075–1090.

Gustafsson, B.G., Westman, P., 2002. On the causes for salinity variations in the Baltic Sea during the last 8500 years. Paleoceanography 17 (3).

Gustafsson, B.G., Schenk, F., Blenckner, T., Eilola, K., Meier, H.E.M., Müller-Karulis, B., Neumann, T., Ruoho-Airola, T., Savchuk, O.P., Zorita, E., 2012. Reconstructing the development of Baltic Sea eutrophication 1850–2006. Ambio 41 (6), 534–548. http://dx.doi.org/10.1007/s13280-012-0318-x.

Hardisty, D.S., Riedinger, N., Planavsky, N.J., Asael, D., Andrén, T., Jørgensen, B.B., Lyons, T.W., 2016. A Holocene history of dynamic water column redox conditions in the Landsort Deep, Baltic Sea. Am. J. Sci. 316 (8), 713–745.

Helz, G.R., Miller, C.V., Charnock, J.M., Mosselmans, J.F.W., Patrick, R.A.D., Garner, D.D., Vaughan, D.J., 1996. Mechanism of molybdenum removal from the sea and its concentration in black shales: EXAFS evidence. Geochim. Cosmochim. Acta 60, 3631–3642.

Henkel, S., Mogollón, J.M., Nöthen, K., Franke, C., Bogus, K., Robin, E., Bahr, A., Blumenberg, M., Pape, T., Seifert, R., März, C., de Lange, G.J., Kasten, S., 2012. Diagenetic barium cycling in Black Sea sediments e a case study for anoxic marine environments. Geochim. Cosmochim. Acta 88, 88–105.

Hennekam, R., Jilbert, T., Mason, P.R., de Lange, G.J., Reichart, G.J., 2015. High-resolution line-scan analysis of resin-embedded sediments using laser ablation-inductively coupled plasma-mass spectrometry (LA-ICP-MS). Chem. Geol. 403, 42–51.

Ingri, J., Widerlund, A., Suteerasak, T., Bauer, S., Elming, S.-Å., 2014. Changes in trace metal sedimentation during freshening of a coastal basin. Mar. Chem. 167, 2–12.

Ip, C.C.M., Li, X.D., Zhang, G., Wai, O.W.H., Li, Y.S., 2007. Trace metal distribution in sediments of the Pearl River Estuary and the surrounding coastal area, South China. Environ. Pollut. 147, 311–323.

Jilbert, T., Slomp, C.P., 2013a. Rapid high-amplitude variability in Baltic Sea hypoxia during the Holocene. Geology 41, 1183–1186. http://dx.doi.org/10.1130/G34804.1.

Jilbert, T., Slomp, C.P., 2013b. Iron and manganese shuttles control the formation of authigenic phosphorus minerals in the euxinic basins of the Baltic Sea. Geochim. Cosmochim. Acta 107, 155–169.

Jilbert, T., de Lange, G., Reichart, G.J., 2008. Fluid displacive resin embedding of laminated sediments: preserving trace metals for high-resolution paleoclimate investigations. Limnol. Oceanogr. Methods 6 (1), 16–22.

Jilbert, T., Conley, D.J., Gustafsson, B.G., Funkey, C.P., Slomp, C.P., 2015. Glacio-isostatic control on hypoxia in a high-latitude shelf basin. Geology 43, 427–430. http://dx.doi.org/10.1130/G36454.1.

Jokinen, S.A., Virtasalo, J.J., Jilbert, T., Kaiser, J., Dellwig, O., Arz, H.W., Hänninen, J., Arppe, L., Collander, C., Saarinen, T., 2018. A 1500-year multiproxy record of coastal hypoxia from the northern Baltic Sea indicates unprecedented deoxygenation over the 20th century. Biogeosciences (in press).

Klinkhammer, G.P., Palmer, M.R., 1991. Uranium in the oceans: where it goes and why. Geochim. Cosmochim. Acta 55, 1799–1806.

Koide, M., Hodge, V.F., Yany, J., Stallard, M., Goldberg, E., Calhoun, J., Bertine, K., 1986. Some comparative marine geochemistries of rhenium, gold, silver and molybdenum. Appl. Geochem. 1, 705–714.

Kremling, K., Streu, P., 2000. Further evidence for a drastic decline of potentially hazardous trace metals in Baltic Sea surface waters. Mar. Pollut. Bull. 40 (8), 674–679.

Lass, H.U., Matthäus, W., 1996. On temporal wind variations forcing salt water inflows into the Baltic Sea. Tellus 48A, 663–671.

Lenz, C., Jilbert, T., Conley, D.J., Slomp, C.P., 2015a. Hypoxia-driven variations in iron and manganese shuttling in the Baltic Sea over the past 8 kyr. Geochem. Geophys. Geosyst. 16 (10), 3754–3766.

Lenz, C., Jilbert, T., Conley, D.J., Wolthers, M., Slomp, C.P., 2015b. Are recent changes in sediment manganese sequestration in the euxinic basins of the Baltic Sea linked to the expansion of hypoxia? Biogeosciences 12, 4875–4894.

Liaghati, T., Preda, M., Cox, M., 2004. Heavy metal distribution and controlling factors within coastal plain sediments, Bells Creek catchment, southeast Queensland, Australia. Environ. Int. 29 (7), 935–948.

Matthäus, W., Franck, H., 1992. Characteristics of major Baltic inflows—a statistical analysis. Cont. Shelf Res. 12 (12), 1375–1400.

McArthur, J.M., Algeo, T.J., van de Schootbrugge, B., Li, Q., Howarth, R.J., 2008. Basinal restriction, black shales, Re–Os dating, and the early Toarcian (Jurassic) oceanic anoxic event. Paleoceanography 23, PA4217. http://dx.doi.org/10.1029/2008PA001607.

McLennan, S.M., 2001. Relationships between the trace element composition of sedimentary rocks and upper continental crust. Geochem. Geophys. Geosyst. 2 (4).

McManus, J., Berelson, W.M., Klinkhammer, G.P., Johnson, K.S., Coale, K.H., Anderson, R.F., Kumar, N., Burdige, D.J., Hammond, D.E., Brumsack, H.J., McCorkle, D.C., Rushdi, A., 1998. Geochemistry of barium in marine sediments: implications for its use as a paleoproxy. Geochim. Cosmochim. Acta 62, 3453–3473.

Mohrholz, V., Naumann, M., Nausch, G., Krüger, S., Gräwe, U., 2015. Fresh oxygen for the Baltic Sea—an exceptional saline inflow after a decade of stagnation. J. Mar. Syst. 148, 152–166. http://dx.doi.org/10.1016/j.jmarsys.2015.03.005.

Morford, J.L., Emerson, S., 1999. The geochemistry of redox sensitive trace metals in sediments. Geochim. Cosmochim. Acta 63 (11), 1735–1750.

Morford, J.L., Emerson, S.R., Breckel, E.J., Kim, S.H., 2005. Diagenesis of oxyanions (V, U, Re, and Mo) in pore waters and sediments from a continental margin. Geochim. Cosmochim. Acta 69, 5021–5032.

Morford, J.L., Martin, W.R., Carney, C.M., 2012. Rhenium geochemical cycling: insights from continental margins. Chem. Geol. 324–325, 73–86.

Nägler, T.F., Neubert, N., Böttcher, M.E., Dellwig, O., Schnetger, B., 2011. Molybdenum isotope fractionation in pelagic euxinia: evidence from the modern Black and Baltic seas. Chem. Geol. 289, 1–11.

Noordmann, J., Weyer, S., Montoya-Pino, C., Dellwig, O., Neubert, N., Eckert, S., Paetzel, M., Böttcher, M.E., 2015. Uranium and molybdenum isotope systematics in modern euxinic basins: case studies from the central Baltic Sea and the Kyllaren fjord (Norway). Chem. Geol. 396, 182–195.

Nriagu, J.O., Pacyna, J.M., 1988. Quantitative assessment of worldwide contamination of air, water and soils by trace metals. Nature 333, 134–139.
O'Connor, A.E., Luek, J.L., McIntosh, H., Beck, A.J., 2015. Geochemistry of redox-sensitive trace elements in a shallow subterranean estuary. Mar. Chem. 172, 70–81.
Olson, L., Quinn, K.A., Siebecker, M.G., Luther, G.W., Hastings, D., Morford, J.L., 2017. Trace metal diagenesis in sulfidic sediments: insights from Chesapeake Bay. Chem. Geol. 452, 47–59.
Papadomanolaki, N.M., Dijkstra, N., Van Helmond, N.A.G.M., Hagens, M., Bauersachs, T., Kotthoff, U., Sangiorgi, F., Slomp, C.P., 2018. Controls on the onset and termination of past hypoxia in the Baltic Sea. Palaeogeogr. Palaeoclimatol. Palaeoecol. 490, 347–354.
Pedersen, T.F., Calvert, S.E., 1990. Anoxia vs. productivity: what controls the formation of organic-carbon-rich sediments and sedimentary rocks? (1). AAPG Bull. 74 (4), 454–466.
Piper, D.Z., Perkins, R.B., 2004. A modern vs. Permian black shale—the hydrography, primary productivity, and water-column chemistry of deposition. Chem. Geol. 206 (3–4), 177–197.
Plewa, K., Meggers, H., Kasten, S., 2012. Barium in sediments off northwest Africa: a tracer for paleoproductivity or meltwater events? Paleoceanography 21. http://dx.doi.org/10.1029/2005PA001136.
Prange, A., Kremling, K., 1985. Distribution of dissolved molybdenum, uranium and vanadium in Baltic Sea waters. Mar. Chem. 16 (3), 259–274.
Schaller, T., Morford, J., Emerson, S., Feely, R., 2000. Oxyanions in metalliferous sediments: tracers for paleoseawater metal concentrations? Geochim. Cosmochim. Acta 63 (13), 2243–2254.
Schinke, H., Matthäus, W., 1998. On the causes of major Baltic inflows — an analysis of long time series. Cont. Shelf Res. 18, 67–97.
Schneider, B., Ceburnis, D., Marks, R., Munthe, J., Petersen, G., Sofiev, M., 2000. Atmospheric Pb and Cd input into the Baltic Sea: a new estimate based on measurements. Mar. Chem. 71, 297–307.
Schoepfer, S.D., Shen, J., Wei, H., Tyson, R.V., Ingall, E., Algeo, T.J., 2015. Total organic carbon, organic phosphorus, and biogenic barium fluxes as proxies for paleomarine productivity. Earth-Sci. Rev. 149, 23–52.
Scott, C., Lyons, T.W., 2012. Contrasting molybdenum cycling and isotopic properties in euxinic versus non-euxinic sediments and sedimentary rocks: refining the paleoproxies. Chem. Geol. 324–325, 19–27.
Shaw, T.J., Gieskes, J.M., Jahnke, R.A., 1990. Early diagenesis in differing depositional environments: the response of transition metals in pore water. Geochim. Cosmochim. Acta 54 (5), 1233–1246.
Sulu-Gambari, F., Roepert, A., Jilbert, T., Hagens, M., Meysman, F.J., Slomp, C.P., 2017. Molybdenum dynamics in sediments of a seasonally-hypoxic coastal marine basin. Chem. Geol. 466, 627–640.
Szefer, P., Szefer, K., Glasby, G.P., Pempkowiak, J., Kaliszan, R., 1996. Heavy metal pollution in surficial sediments from the southern Baltic Sea off Poland. J. Environ. Sci. Health A 31 (10), 2723–2754.
Tribovillard, N., Algeo, T.J., Lyons, T., Riboulleau, A., 2006. Trace metals as paleoredox and paleoproductivity proxies: an update. Chem. Geol. 232 (1), 12–32.
Tribovillard, N., Algeo, T.J., Baudin, F., Riboulleau, A., 2012. Analysis of marine environmental conditions based onmolybdenum–uranium covariation—applications to Mesozoic paleoceanography. Chem. Geol. 324, 46–58.
Turekian, K.K., 1977. The fate of metals in the oceans. Geochim. Cosmochim. Acta 41 (8), 1139–1144.
van Helmond, N.A.G.M., Ruvalcaba Baroni, I., Sluijs, A., Sinninghe Damsté, J.S., Slomp, C.P., 2014. Spatial extent and degree of oxygen depletion in the deep proto-North Atlantic Basin during Oceanic Anoxic Event 2. Geochem. Geophys. Geosyst. 15 (11), 4254–4266.
van Helmond, N.A.G.M., Quintana Krupinski, N.B., Lougheed, B.C., Obrochta, S.P., Andrén, T., Slomp, C.P., 2017. Seasonal hypoxia was a natural feature of the coastal zone in the Little Belt, Denmark, during the past 8 ka. Mar. Geol. 387, 45–57.
Von Breymann, M.T., Emeis, K.-C., Suess, E., 1992. Water depth and diagenetic constraints on the use of barium as a palaeoproductivity indicator. Geol. Soc. Lond. Spec. Publ. 64, 273–284.
Wanty, R.B., Goldhaber, R., 1992. Thermodynamics and kinetics of reactions involving vanadium in natural systems: accumulation of vanadium in sedimentary rock. Geochim. Cosmochim. Acta 56, 171–183.
Wehrli, B., Stumm, W., 1989. Vanadyl in natural waters: adsorption and hydrolysis promote oxygenation. Geochim. Cosmochim. Acta 53, 69–77.
Windom, H.L., Schropp, S.J., Calder, F.D., Ryan, J.D., Smith Jr., R.G., Burney, L.C., Lewis, F.G., Rawlinson, C.H., 1989. Natural trace metal concentrations in estuarine and coastal marine sediments of the southeastern United States. Environ. Sci. Technol. 23, 314–320.
Zheng, Y., Anderson, R.F., van Geen, A., Fleisher, M.Q., 2002. Preservation of non-lithogenic particulate uranium in marine sediments. Geochim. Cosmochim. Acta 66, 3085–3092.
Zillén, L., Conley, D.J., Andrén, T., Andrén, E., Björck, S., 2008. Past occurrences of hypoxia in the Baltic Sea and the role of climate variability, environmental change and human impact. Earth Sci. Rev. 91, 77–92. http://dx.doi.org/10.1016/j.earscirev.2008.10.001.
Zillén, L., Lenz, C., Jilbert, T., 2012. Stable lead (Pb) isotopes and concentrations – a useful independent dating tool for Baltic Sea sediments. Quat. Geochronol. 8, 41–45.